

## Durham Research Online

---

### Deposited in DRO:

25 January 2011

### Version of attached file:

Published Version

### Peer-review status of attached file:

Peer-reviewed

### Citation for published item:

Brand, S. and Kaliteevski, M.A. and Abram, R.A. (2006) 'THz frequency studies of metallic structures.', Proceedings of SPIE., 6328 . p. 63280.

### Further information on publisher's website:

<http://dx.doi.org/10.1117/12.680313>

### Publisher's copyright statement:

Copyright 2006 Society of Photo-Optical Instrumentation Engineers. One print or electronic copy may be made for personal use only. Systematic electronic or print reproduction and distribution, duplication of any material in this paper for a fee or for commercial purposes, or modification of the content of the paper are prohibited.

### Additional information:

## Use policy

---

The full-text may be used and/or reproduced, and given to third parties in any format or medium, without prior permission or charge, for personal research or study, educational, or not-for-profit purposes provided that:

- a full bibliographic reference is made to the original source
- a [link](#) is made to the metadata record in DRO
- the full-text is not changed in any way

The full-text must not be sold in any format or medium without the formal permission of the copyright holders.

Please consult the [full DRO policy](#) for further details.

# THz frequency studies of metallic structures

S. Brand\*, M. A. Kaliteevski and R. A. Abram

Physics Dept., Rochester Building, Science Labs., Durham University, South Road, Durham,  
DH1 3LE, U.K.

## ABSTRACT

A plane-wave complex photonic bandstructure approach is used to calculate the pass bands as a function of rod diameter for a system consisting of circular metallic rods in a 2-D square lattice. In addition, FDTD calculations are employed to calculate the transmission properties of a finite 6-layer structure of the same form. The results of the two methods are compared and found to be consistent. The effective plasma frequency, the lowest frequency at which propagation can occur in the infinite lattice, is extracted from the bandstructure calculations, and is in the region of 1 THz for the 200  $\mu\text{m}$  period structures considered. The results for the effective plasma frequency are compared to those predicted by several analytic models.

**Keywords:** Photonic bandstructure, plasma frequency, THz

## 1. INTRODUCTION

Some time ago Pendry et al<sup>1,2</sup> studied the problem of low frequency plasmons in thin wire structures and proposed a simple analytic theory to explain the principal feature characterizing their low frequency response to incident electromagnetic radiation in the case of a periodic 2-D arrangement of such wires: the existence of an effective plasma frequency below that of the bulk metallic value. In their thin wire model, which is notable for the fact that the result depends only on geometrical factors and not the bulk plasma frequency, the effective plasma frequency is given by:

$$\omega_{p,\text{eff}}^2 = \frac{2\pi c^2}{a^2 \ln(a/r)} \quad (1)$$

where  $a$  is the lattice constant,  $r$  is the radius of the rods and  $c$  the free-space velocity of light. In practice, no propagation can occur in the infinite structure below the effective plasma frequency, in analogy with the related effect in bulk material. Since the work of Pendry et al a number of alternative simple analytic expressions for the effective plasma frequency have been proposed<sup>3,4,5</sup>. There have also been various other theoretical studies of both the photonic bandstructure for infinite systems<sup>6,7</sup> and transmission calculations in the case of finite structures<sup>8,9</sup>. Experimental results have been reported both in the original work of Pendry et al<sup>2</sup> and also, more recently, by Pimenov and Loidl<sup>10</sup> who investigated arrays of copper and steel wires using broadband terahertz spectroscopy.

It should be noted that the effective plasma frequency model only applies in the situation where the electric field is polarized parallel to the direction of the axis of the rods (we shall refer to this as TM polarization). For the alternative TE polarization, in which the magnetic field is parallel to the rods, the effective plasma frequency model does not apply and the results are rather similar to those expected for a standard dielectric photonic bandgap structure, apart from the existence of additional, effectively dispersionless, localized plasmon states essentially confined to the surface of individual rods<sup>6,11</sup>.

In the present work, in Section 2, we present brief details concerning a general 2-D plane-wave complex photonic bandstructure method. The method is then applied to a particular structure consisting of circular metallic rods in a square lattice, with results presented in Section 3.1. Section 3.2 describes a more general set of numerical results and compares them to the predictions of various analytic theories for the effective plasma frequency that have been reported in the literature, and compares these to our results. Our conclusions are presented in Section 4.

## 2. THEORY OUTLINE

In a standard 2-D plane-wave photonic bandstructure formulation as described by for example Plihal and Maradudin<sup>12</sup> the wavevector  $\underline{k}$  is fixed and it is then possible to calculate the frequency as a function of  $\underline{k}$  throughout the Brillouin zone. This approach, however, only works provided that the structure has no components with a frequency-dependent permittivity, and is therefore not really applicable to metallic structures. An extension to the method allowing a frequency-dependent permittivity to be used, was later described by Kuzmiak et al<sup>6</sup> but nevertheless this only applies to a permittivity of the specific form  $\varepsilon(\omega) = 1 - \omega_p^2 / \omega^2$ . In practice, we would prefer to be able to deal with any general frequency-dependent form for the permittivity, of any component in the structure, possibly including absorption, and this can be achieved by employing a complex bandstructure formalism. Full details of our approach for both TM and TE polarizations are given elsewhere<sup>13</sup> so in what follows we shall confine ourselves to giving only an outline of the method for the case of TM polarization, the polarization of interest for the present work.

We begin by assuming a 2-D periodic structure of the form shown in Fig. 1, although any more general cross-section is possible.

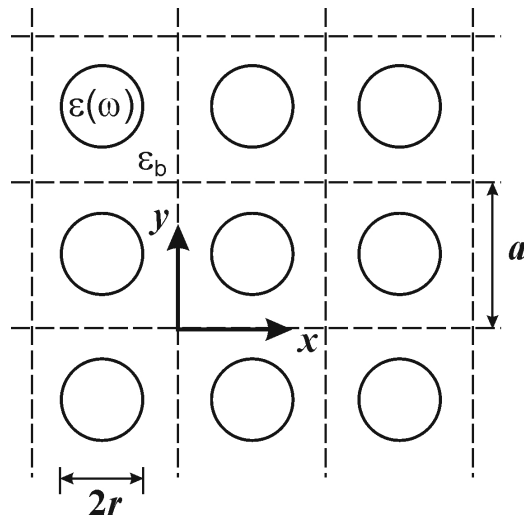


Fig.1 An array of circular rods having a frequency-dependent relative permittivity  $\varepsilon(\omega)$  embedded in a background material for which the relative permittivity has a constant value  $\varepsilon_b$ .

The permittivity is represented in the form

$$\varepsilon(x, y) = \varepsilon(\underline{\rho}) = \varepsilon_b + [\varepsilon(\omega) - \varepsilon_b] S(\underline{\rho})$$

where  $S(\underline{\rho}) = 1$  within the rods and  $S(\underline{\rho}) = 0$  elsewhere. We use the Fourier series expansions over reciprocal lattice vectors

$$S(\underline{\rho}) = \sum_{\underline{g}'} S_{\underline{g}'} e^{i\underline{g}' \cdot \underline{\rho}} \quad , \quad E_z(\underline{\rho}) = \sum_{\underline{g}} E_{\underline{g}} e^{i(\underline{k} + \underline{g}) \cdot \underline{\rho}}$$

for  $S(\underline{\rho})$  and the electric field in the  $z$  direction respectively. Insertion of the above into Maxwell's equations eventually leads to a matrix equation

$$\begin{pmatrix} 0 & I \\ C-B & -A \end{pmatrix} \begin{pmatrix} \underline{E} \\ k\underline{E} \end{pmatrix} = k \begin{pmatrix} \underline{E} \\ k\underline{E} \end{pmatrix} \quad (2)$$

for a general complex wavevector  $\underline{k} = k\underline{\hat{u}}$  in the  $x$ - $y$  plane,  $\underline{\hat{u}}$  being a unit vector in the direction of the wavevector and  $\underline{E}$  is a vector whose components are the expansion coefficients  $E_{\underline{g}}$ .

In (2), if  $n$  plane-waves are used in the  $E$  - field expansion, the various  $n \times n$  sub-matrices are such that

$I$  is the identity matrix

$A$  has only diagonal elements given by  $A_{\underline{g},\underline{g}} = 2\underline{G} \cdot \underline{\hat{u}}$

$B$  has only diagonal elements given by  $B_{\underline{g},\underline{g}} = G^2 - \frac{\omega^2}{c^2} \varepsilon_b$

$C$  has the elements  $C_{\underline{g},\underline{g}} = \frac{\omega^2}{c^2} [\varepsilon(\omega) - \varepsilon_b] S_{\underline{g}-\underline{g}}$ .

Knowing the form of  $\varepsilon(\omega)$  we can then scan through frequency in order to determine  $k$ , and thus the whole complex bandstructure of the system can be mapped out. As (2) involves a  $2n \times 2n$  general complex matrix with general complex eigenvalues this process is somewhat more time-consuming than standard plane-wave bandstructure calculations.

### 3. RESULTS

We now consider a series of 200  $\mu\text{m}$  lattice constant arrays containing gold rods with a range of diameters from 10  $\rightarrow$  120  $\mu\text{m}$ , with specific detailed results for a 50  $\mu\text{m}$  diameter rod structure presented in Section 3.1 and more general results for the effective plasma frequency as a function of rod diameter presented in Section 3.2. Experimental colleagues are currently fabricating finite layer versions of such structures and detailed results for the transmission properties will be available in due course. For our calculations we take the background permittivity to be that for air,  $\varepsilon_b = 1$ , and to represent the permittivity of the gold rods we employ the Drude expression

$$\varepsilon(\omega) = 1 - \frac{\omega_p^2}{\omega(\omega + i\omega_c)}$$

where values  $\omega_p = 2\pi \times 2.175 \times 10^{15} \text{ s}^{-1}$ , for the bulk plasma frequency for gold,  $\omega_c = 2\pi \times 6.5 \times 10^{12} \text{ s}^{-1}$ , the absorption term, are taken from Ordal et al<sup>14</sup>.

#### 3.1 Square lattice with 200 $\mu\text{m}$ lattice constant and 50 $\mu\text{m}$ diameter gold rods

As an example of the form of the resultant bandstructure we show representative results for an array of 50  $\mu\text{m}$  diameter rods in Fig. 2. The calculations were for wavevectors in a [100] direction and employed 805 plane waves for the  $E$  - field expansion and in this case the absorption term has been omitted. The figure shows the existence of two purely imaginary  $k$ , evanescent, solutions over the range of frequencies displayed. Also shown is an initially evanescent solution with  $\text{Im}(k) \approx 0.5 \times (2\pi/a)$  at low frequencies which evolves into a purely real solution, indicating the value of the effective plasma frequency, close to 0.67 THz, and giving rise to a pass band up to about 0.84 THz. A second pass band is present from about 1.16  $\rightarrow$  1.53 THz and a band gap region, corresponding to general complex wavevector, with  $\text{Re}(k) = 0.5 \times (2\pi/a)$  is to be seen in the region between the two pass bands. At the centre of this band gap region, at  $\approx 1$  THz, we have that  $\text{Im}(k) \approx 0.15 \times (2\pi/a)$  corresponding to an  $E$  - field decay length of about one lattice constant. This indicates that for any finite structure consisting of more than a few layers there will be negligible transmission at frequencies corresponding to the centre of the band gap region. At higher frequencies not shown in the figure the bandstructure becomes more complicated with additional pass and stop bands.

Although we do not give graphical results here, our calculations show that with the inclusion of the absorption term,  $\omega_c$ , all wavevectors become of general complex form and come in  $\pm k$  pairs. However, in the regions of the two pass bands,  $\text{Im}(k)$  is relatively small and consistent with electromagnetic wave decay in passing through the structure in the direction given by the sign of the group velocity in the respective band. The value of  $\text{Im}(k)$  is such that the  $E$  - field decay length is about 15 periods at the centre of the first “pass band” and about 25 periods for the second band. The decay length at frequencies corresponding to the central region between these two bands is little affected by the inclusion of the absorption term. We note that the results are not particularly sensitive to the value of  $\omega_c$ , and similar decay lengths within the bands are obtained even with significantly larger values of  $\omega_c$ .

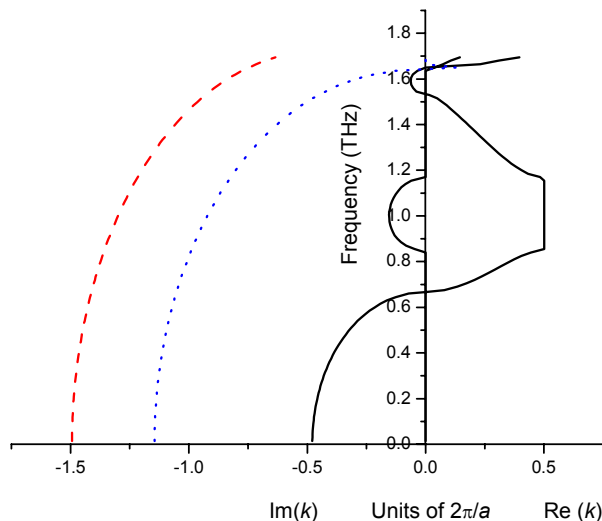


Fig. 2 Complex bandstructure of an array of 50  $\mu\text{m}$  gold rods in a 200  $\mu\text{m}$  period square lattice. The dashed and dotted lines correspond to purely imaginary wavevector solutions. The solid line indicates evanescent, purely imaginary, solutions in the region up to the effective plasma frequency at about 0.67 THz. Pass bands, corresponding to purely real  $k$  are present in the ranges from about 0.67 $\rightarrow$ 0.84 THz and 1.16 $\rightarrow$ 1.53 THz with general complex solutions indicating a band gap region in between. There is no special significance to the sign of  $\text{Im}(k)$  and  $\text{Re}(k)$  in this plot, which is chosen purely for plotting convenience.

In order to consider the transmission properties further we have also performed FDTD studies of the 50  $\mu\text{m}$  diameter rod - 200  $\mu\text{m}$  lattice constant structure. In particular, we have calculated the transmission for a 6-layer structure and the results of these calculations are shown in Fig. 3. The calculations were performed by directing a short pulse of EM radiation at the structure and comparing the Fourier transforms of the incident and transmitted signals. There are inherent numerical errors in this process as can be seen by the peak value of the transmission, which exceeds unity. We note that similar deconvolution errors are also to be expected in any experimental analysis as actual THz pulses tend to have a fairly complicated profile.

The most notable feature in the calculated transmission spectrum is the large, broad peak centred at about 1.34 THz. The position of this peak corresponds almost exactly with the centre of the second pass band found in the bandstructure calculations. The smaller lower frequency peak, at about 0.83 THz, is slightly above the centre of the first band seen in the bandstructure calculations but both calculations are in agreement with regard to the existence of a lower frequency, narrower width band at these lower frequencies. In practice, due to the finite size of the structure employed for the transmission calculations, we would expect to encounter some differences. Although not fully shown in Fig. 2 we note that the bandstructure calculations also reveal other pass bands at about 1.64 $\rightarrow$ 1.72 THz and 1.9 $\rightarrow$ 2.2 THz and in the region above 2.35 THz. We would not expect the first of these bands to be particularly distinguishable in transmission because, as can be seen in Fig. 2, the value of  $\text{Im}(k)$  is quite small in the region between bands 2 and 3 – in effect this band appears to turn up as a shoulder to the main peak. The FDTD transmission peak at 1.98 THz and the onset of

further significant transmission above 2.3 THz are both consistent with the bandstructure calculations. We also note that the minima in the transmission results at both  $\approx 1.75$  THz and just under 1 THz correspond almost exactly with peak values of  $\text{Im}(k)$  in the bandstructure calculations. Overall, we believe that that our results demonstrate good agreement between the bandstructure and FDTD transmission results.

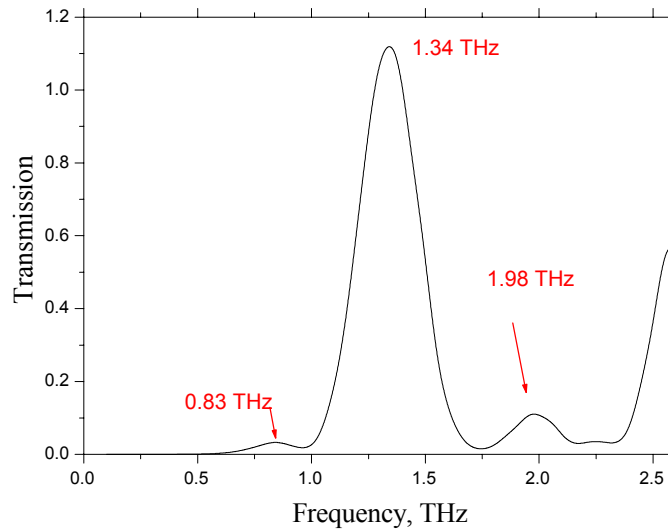


Fig. 3 Plot showing the transmission for a finite structure consisting of 6 layers of 50  $\mu\text{m}$  diameter gold rods in a 200  $\mu\text{m}$  lattice constant array. The FDTD approach is employed to calculate the transmission.

### 3.2 The effective plasma frequency as a function of rod diameter

In this section we neglect the absorption term and show, in Fig. 4, the positions of the first two pass bands obtained from the bandstructure calculations as a function of rod diameter. In all cases the lattice constant is 200  $\mu\text{m}$ .

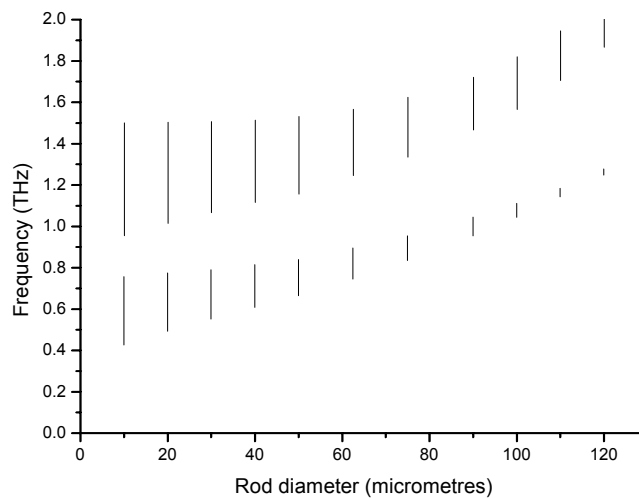


Fig. 4 The location of the first two pass bands as function of rod diameter.

To obtain the results displayed in Fig. 4 we have employed 877 plane waves for the electric field expansion and hence the eigenvalue equation to be solved in (2) has a matrix size of 1754 x 1754.

We note that although there is an order of magnitude change in the rod diameter, and a much larger change in metallic fill factor ( $f$ ), the position of the bands is not greatly altered. The centre of the first band shifts from about 0.6 THz to just over 1 THz, and the centre of the second band shifts from about 1.2 THz to 1.7 THz, following an increase in rod diameter from 10  $\mu\text{m}$  to 100  $\mu\text{m}$ . In practice, if the absorption term in the Drude expression is included, there is little overall difference in the bandstructure but it becomes somewhat problematic to define precisely the positions of the band edges and hence the effective plasma frequency because all solutions are generally complex. However, the basic form of the results is very similar so we define the effective plasma frequency as that at which we first observe the appearance of purely real  $k$  solutions, at the lower edge of the first pass band, without the absorption term.

In Fig. 5 we show a plot of the effective plasma frequency as obtained by the above procedure from our plane-wave calculations compared with the curves obtained from the analytic expressions given by Pendry et al<sup>1,2</sup>, eqn. (1),

Sarychev and Shalaev<sup>3</sup>,

$$\omega_{p,eff}^2 = \frac{2\pi c^2}{a^2 \left\{ \ln \left[ \sqrt{2}a/r \right] + \pi/2 - 3 \right\}}$$

Maslovski et al<sup>4</sup>,

$$\omega_{p,eff}^2 = \frac{2\pi c^2}{a^2 \ln \left[ a^2 / (4ar - 4r^2) \right]}$$

and Tretyakov<sup>5</sup>

$$\omega_{p,eff}^2 = \frac{2\pi c^2}{a^2 \left\{ \ln \left[ a / (2\pi r) \right] + 0.5275 \right\}}$$

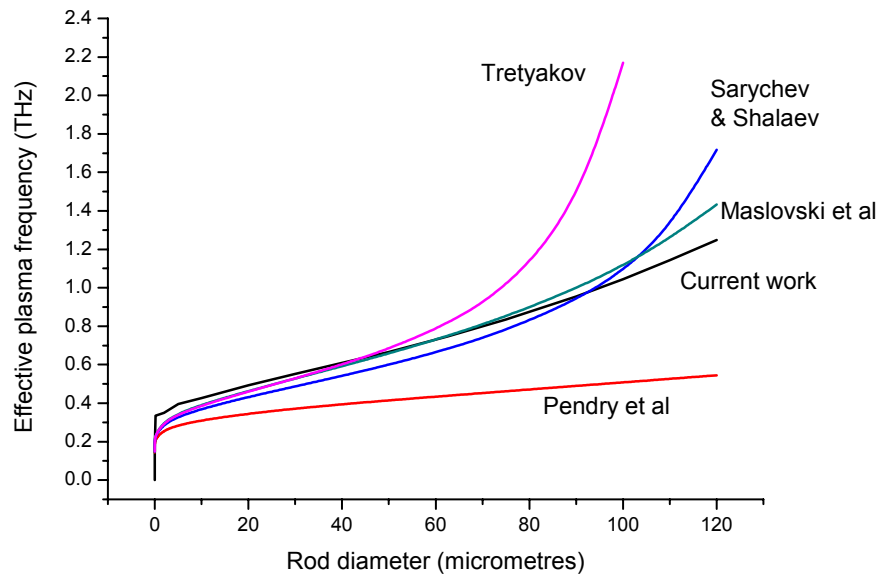


Fig. 5 The effective plasma frequency as a function of rod diameter as obtained from the current plane-wave calculations and as given by various simple analytic models.

The results shown in Fig. 5 make it clear that the Pendry et al expression, which was explicitly obtained for a system of *thin* wires, of much smaller diameter than the rods considered here, does not give particularly good agreement with the plane-wave calculations. Overall, the best agreement is provided by the expression of Maslovski et al, although that of Sarychev and Shalaev also works well. The Tretyakov expression gives results in good agreement with our results at lower frequencies but is much worse as the rod diameter is increased. We note that our calculations cannot be considered to be reliable for rod diameters much below 10  $\mu\text{m}$  due to the number of plane waves employed. Nevertheless, in performing calculations for very small diameter systems we note that the results obtained are in agreement with the expression  $\omega_{p,\text{eff}}^2 = f\omega_p^2$ . In this regime our calculations perform in effect as if we have a uniform system characterised by the average electron concentration, and all structural detail is lost.

With regard to our plane-wave calculations, it should be pointed out that the convergence is such that the results are likely to have an error of a few percent, with the actual effective plasma frequency probably being slightly lower than indicated in Figs. 4 and 5. This convergence problem is inherent to plane-wave calculations and does not have any significance with regard to our basic conclusions, nor is it likely to have any implications when using our method to compare with experimental results. We have also carried out conventional  $\omega(k)$  plane-wave calculations employing a large and constant negative value for the permittivity of the gold rods and although these do reveal the existence of pass bands in somewhat similar positions, the convergence is significantly worse than in the current complex bandstructure calculations. In practice, calculations have also been carried out for structures with the parameters given by Pimenov and Loidl<sup>10</sup> and our results for the positions of the first pass band appears to be in good agreement with their reported experimental results, confirming that convergence is adequate. This experimental work used somewhat larger period structures with lattice constants of 0.45 to 0.9 mm but rather similar fill factors.

#### 4. CONCLUSIONS

We have presented results obtained from calculations of the complex photonic bandstructure of a set of metallic rod structures. Specific comparison of the bandstructure results and those of FDTD calculations appear to demonstrate good agreement for a particular example of one of the systems. In considering a series of structures with differing rod diameters we find good overall agreement with the simple analytic theory of Maslovski et al<sup>4</sup> for the effective plasma frequency. The THz range pass bands displayed in our results may be of practical use for THz filter applications.

#### ACKNOWLEDGEMENTS

MAK acknowledges the financial assistance of EPSRC (UK), grant no. EP/C534263

#### REFERENCES

1. J. B. Pendry, A. J. Holden, A.J. Stewart and I Youngs, Phys. Rev. Lett. 76, 4773 (1996)
2. J. B. Pendry, A. J. Holden, D. J. Robbins and W. J. Stewart, J. Phys.:Condens. Matter 10, 4785 (1998)
3. A.K. Sarychev and V.M. Shalaev, e-print cond-mat/ 0103145 (2001)
4. S. I. Maslovski, S. A. Tretyakov and P. A. Belov, Microwave Opt. Technol Lett., 35, 47 (2002)
5. S. Tretyakov, *Analytical Modeling in Applied Electromagnetics*, Artech House Publishing (2004)
6. V. Kuzmiak, A. A. Maradudin and F. Pincemin, Phys. Rev. B23 16835 (1994)
7. K. Sakoda et al, Phys. Rev. B64 045116 (2001)
8. M. M. Sigalas, C. T. Chan, K. M. Ho and C. M. Soukoulis, Phys. Rev. B16 11744 (1995)
9. P. Markos and C. M. Soukoulis, Opt. Lett. 28, 846 (2003)
10. A. Pimenov and A. Loidl, Phys. Rev. Lett. 96, 063903 (2006)
11. T. Ito and K. Sakoda, Phys. Rev. B64 045117 (2006)
12. M. Plihal and A. A. Maradudin, Phys. Rev. B44 8565 (1991)
13. Submitted for publication